pyValEIA

Alanah Cardenas-O'Toole[1,2], Angeline G. Burrell[3], and Dustin Hickey[3]

[1]University of Michigan

[2]Naval Research Enterprise Internship Program (NREIP)

[3]Naval Research Laboratory

NREIP NAVAL RESEARCH ENTERPRISE INTERNSHIP PROGRAM

U.S. NAVAL RESEARCH LABORATORY

Background

- pyValEIA is a python package created to characterize the 2D shape of the low-latitude ionosphere plasma for observation-model comparison.
- Generally, the Equatorial Ionization Anomaly (EIA) is a double peak structure with a minimum at the magnetic equator.
- The EIA is a result of **E×B** drift and plasma diffusion with hemispheric asymmetries resulting primarily from neutral winds.
- The goal of pyValEIA is to diagnose the physics-based weaknesses of a model using the presence or absence of the EIA.

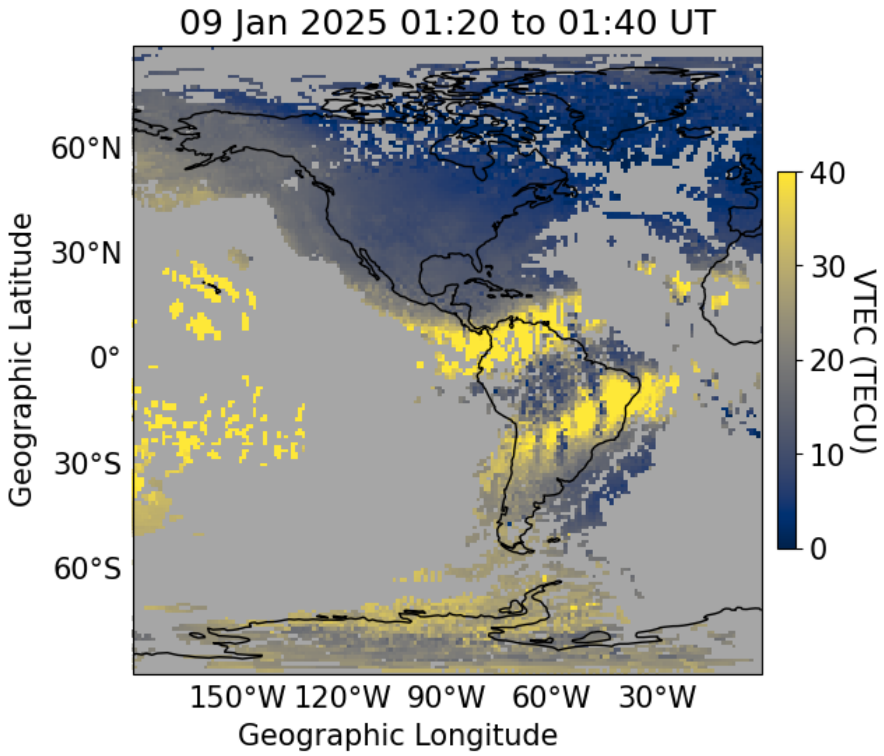

Datasets

- For this study, two periods were chosen: January 2014 and April 2020.
- Swarm A, B, and C
  - Provide 2 Hz in situ plasma density measurements from the Langmuir probes on the Electric Field Instrument (EFI) (Knudsen et al., 2017) at altitudes between 460 km and 511 km.
- Next-Generation Ionosphere Model for Operations (NIMO)
  - Global data assimilative model that uses SAMI3 as the physics-based ionosphere (Burrell et al., 2026).
- PyIRI
  - Pure Python implementation of the International Reference Ionosphere (IRI), is set as the standard comparison for NIMO (Forsythe et al., 2024).
- Madrigal TEC
  - The MIT Haystack Madrigal database provides the Vertical TEC (VTEC) measurements.

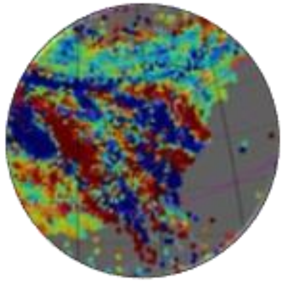

Categories

Equatorial Region Characterization Chart		
Category	**Class**	**Orientation**
Trough		
Flat		North Symmetric South
Peak		North Symmetric South
EIA	Classic	North Symmetric South
	Saddle	North Symmetric South
	Ghost	North Peak North Symmetric South Peak South

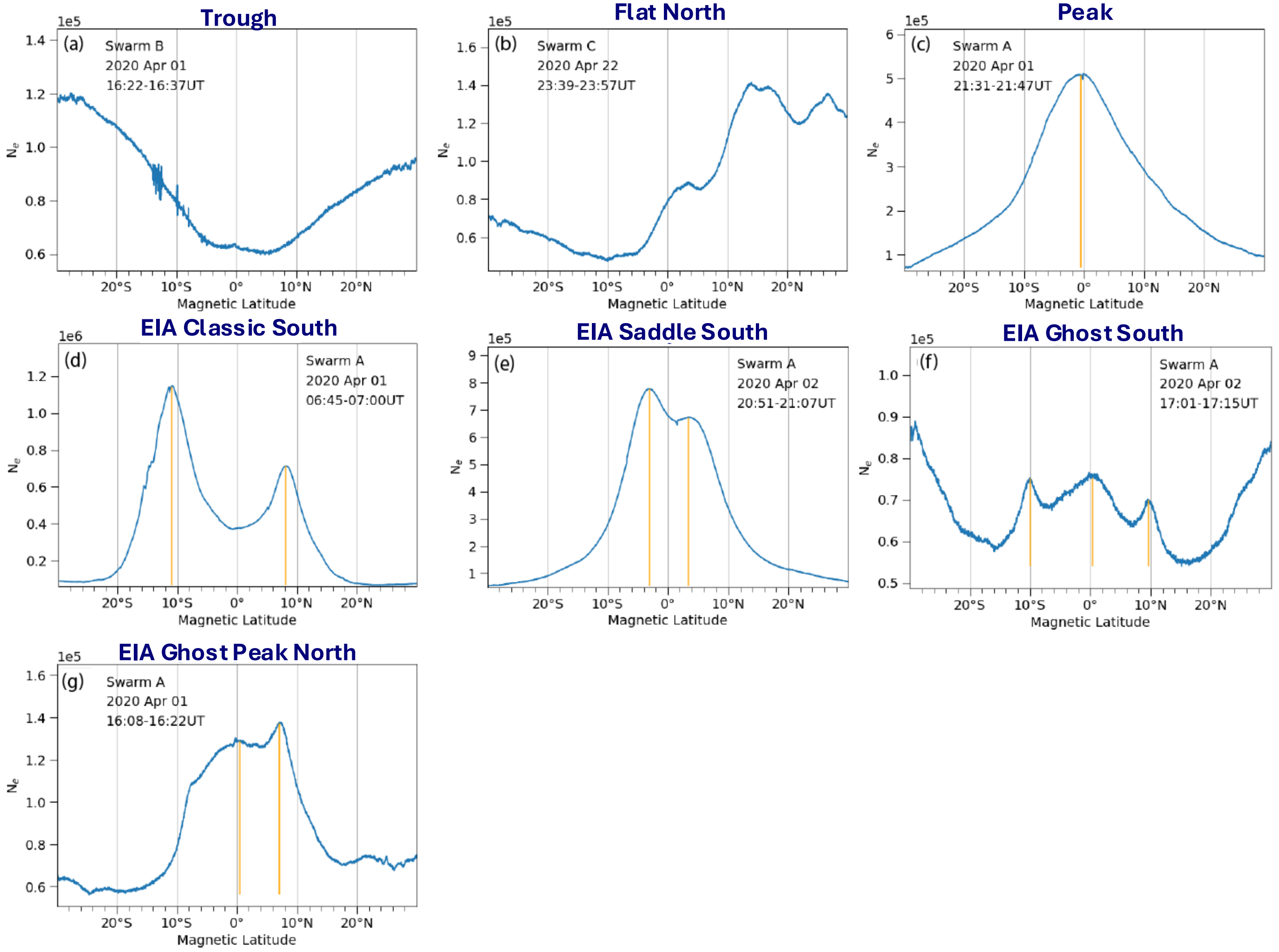

pyValEIA Overview

- The plasma density is processed depending on the density type and cadence.
- The density is scaled so that N_e and TEC can be evaluated in the same system.
- The zero-lats are latitudes where the gradient of the density is zero.
- The zero-lats are designated as maxima and minima.
- The maxima determine the number of crests to detect the category.

$$N_{P_{sc}} = \frac{N_P}{max(N_P)} * [max(MLat) - min(MLat)]$$

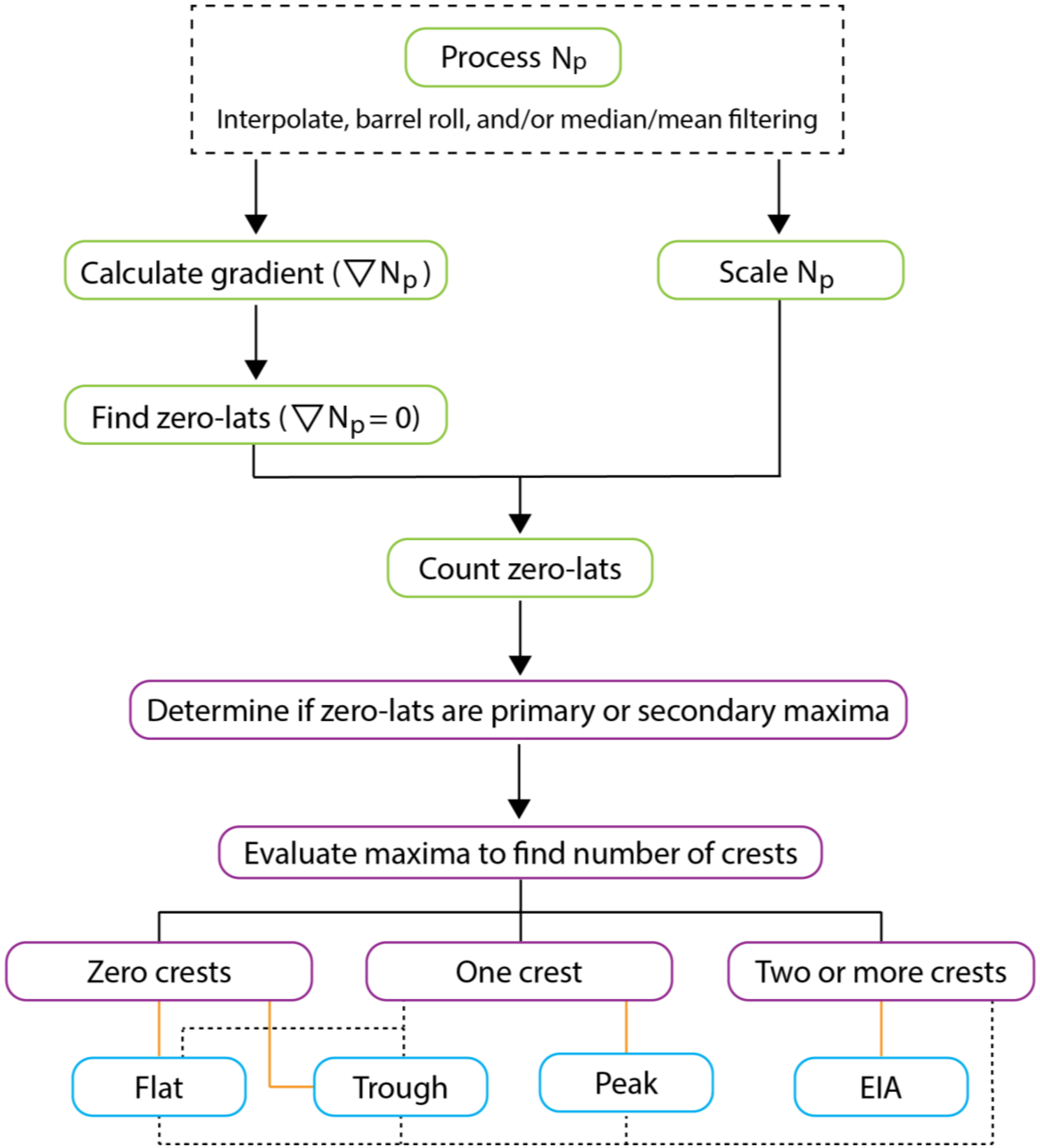

pyValEIA Example

- There are three zero-lats.
- The slopes between the zero-lats and anchors are calculated.
- Zero-lats are designated as primary (diamond) or secondary (square) maxima and minima (circle).
- There are two crests, which are evaluated by their distance, width, and slopes to the minima resulting in an EIA Saddle South designation.

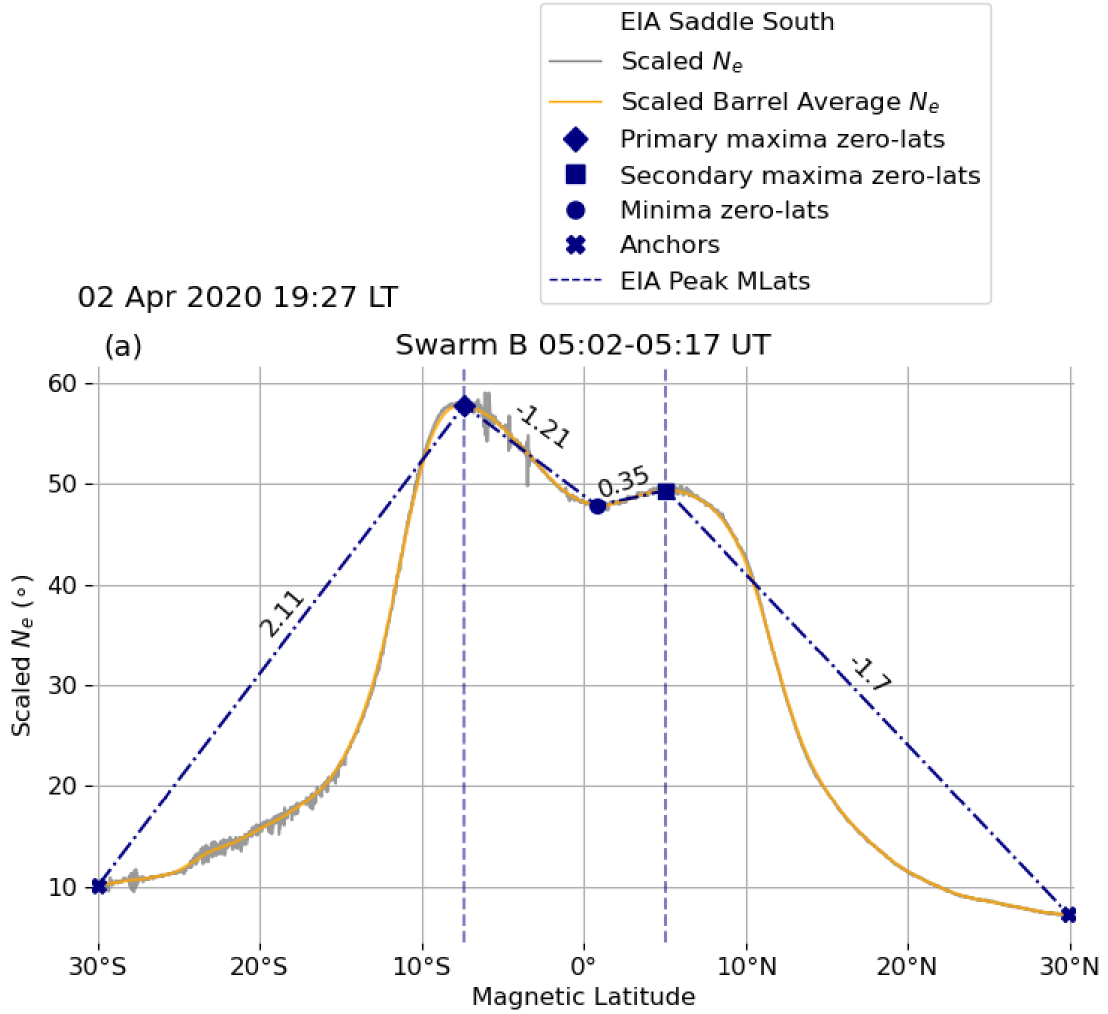

$$N_{P_{sc}} = \frac{N_P}{max(N_P)} * [max(MLat) - min(MLat)]$$

Electron Density

- Swarm N_e data is cleaned, detrended, and smoothed.
- NIMO density data corresponds to the closest time, longitude, and altitude to the Swarm pass.
- PyIRI is chosen as the standard for comparison to NIMO
- Both PyIRI and NIMO are linearly interpolated.

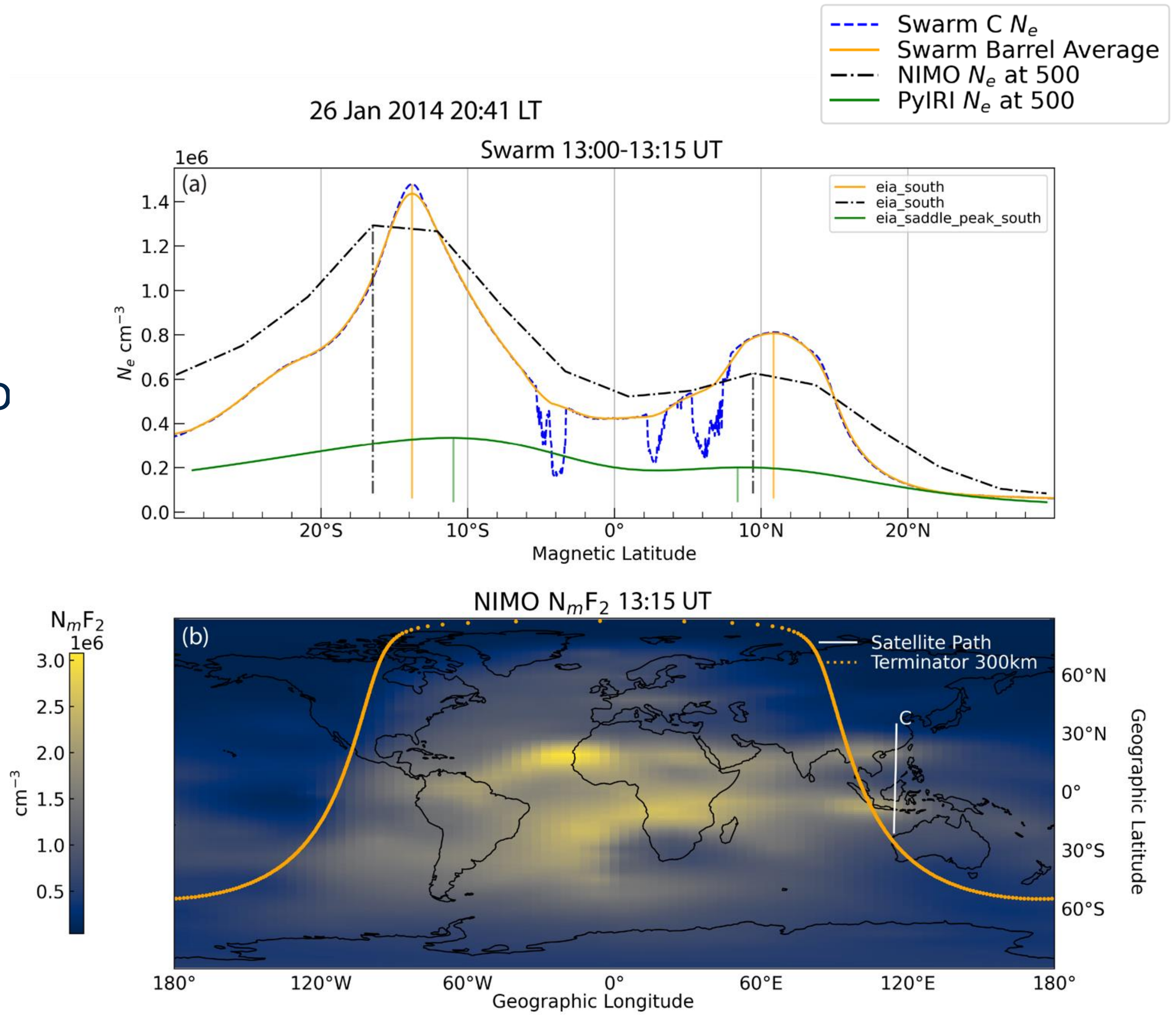

Total Electron Content

- Madrigal TEC measurements are sparse in certain longitudinal sectors
- Two regions were chosen for analysis
  - The American sector: 90°W to 30°W
  - The Asian sector: 60°E to120°E
- The TEC data was binned by 5° longitudes in 15-minute intervals, linearly interpolated, detrended, and smoothed
- NIMO TEC is limited by the TEC longitude and is linearly interpolated

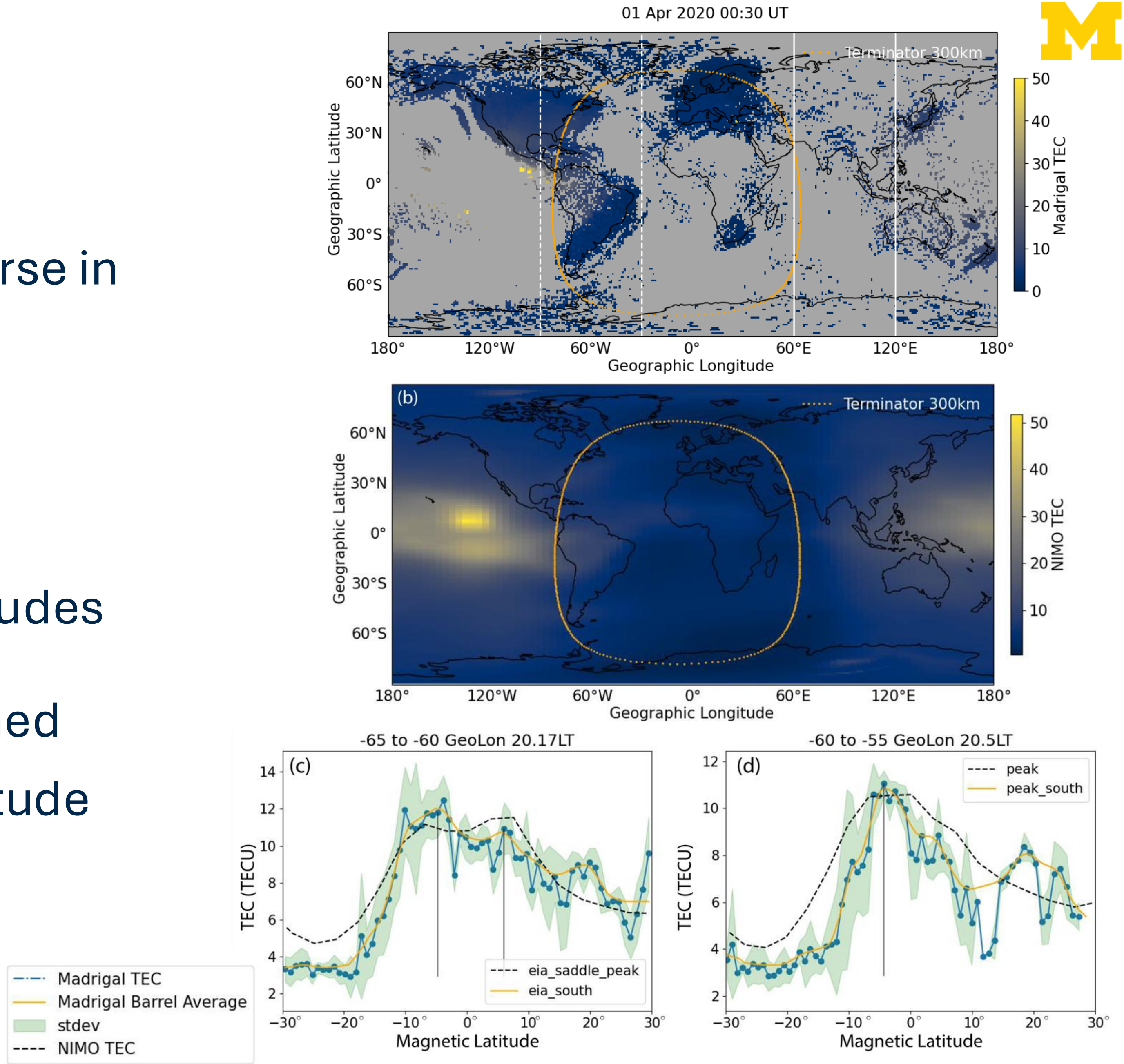

NIMO-PyIRI Comparison

- pyValEIA provides an apples-to-apples comparison between models.
- NIMO has fewer hits and more misses in the African sector indicating under-prediction.
- PyIRI has more hits in the African sector but also more false positives indicating over-prediction of the EIA.

		Observation	
		EIA	non-EIA
Model	EIA	Hit (H)	False Positive (F)
	non-EIA	Miss (M)	Correct Negative (C)

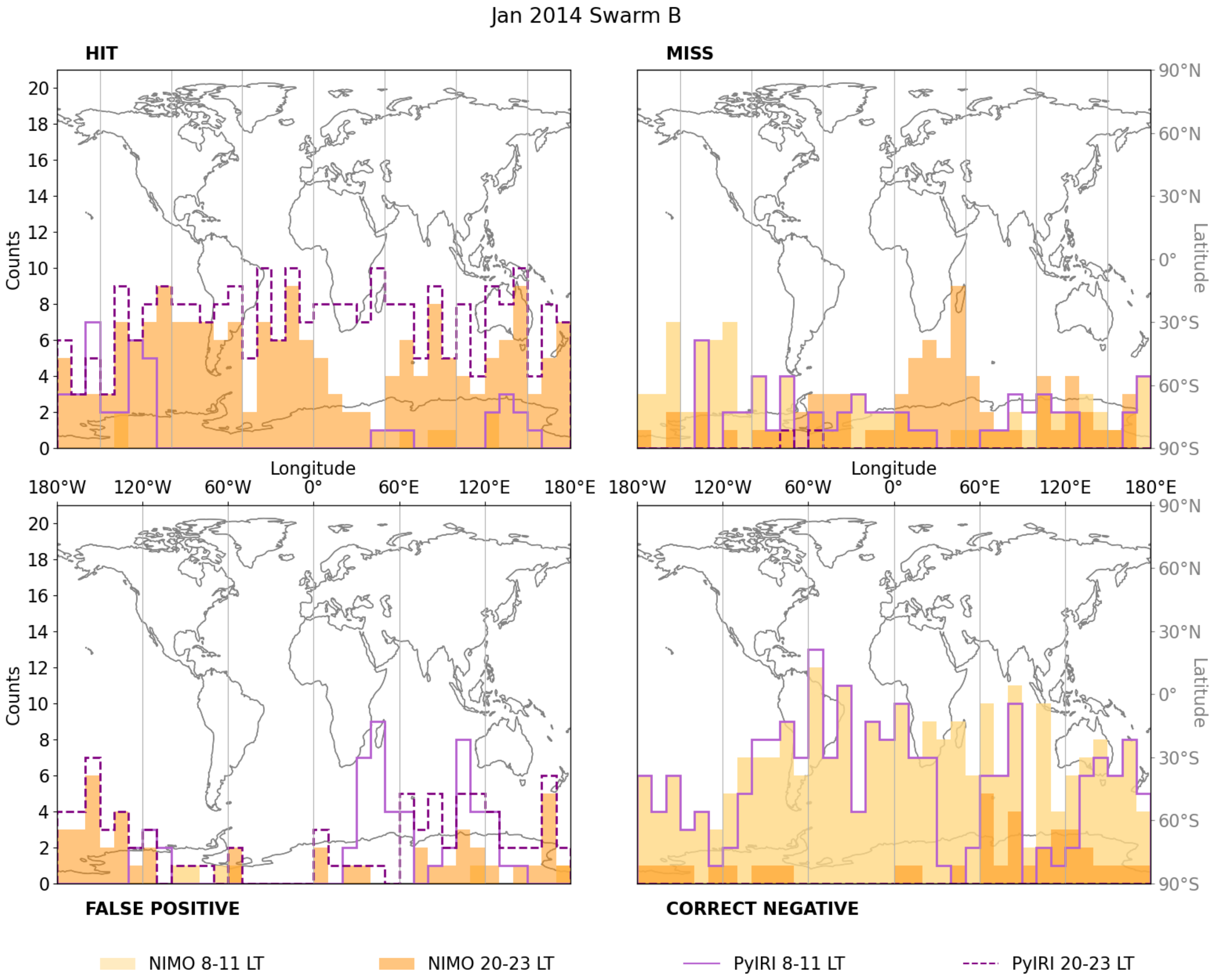

Conclusion

- pyValEIA is designed to categorize the low-latitude ionosphere state based on the presence or absence of the EIA.
- It provides the EIA state, crest latitudes, and crest densities.
- It is useful for statistical data studies, diagnosing weaknesses in models, and performing model-to-model comparisons.
- We demonstrated the use of pyValEIA in TEC and electron density, and we compared between NIMO and PyIRI showing weaknesses and strengths in both.
- pyValEIA is a Python package on GitHub that is in active development.
  - Upcoming releases will include bug-fixes and package enhancements
  - We encourage you to test it and provide feedback!
  - https://github.com/aburrell/pyValEIA

Questions?

Acknowledgements

AGB and DAH are supported by the Office of Naval Research

GPS TEC data products and access through the Madrigal distributed data system are provided to the community by the Massachusetts Institute of Technology under support from US National Science Foundation grant AGS-1952737. Data for the TEC processing is provided from the following organizations UNAVCO, Scripps Orbit and Permanent Array Center, Institut Geographique National, France, International GNSS Service, The Crustal Dynamics Data Information System (CDDIS), National Geodetic Survey, Instituto Brasileiro de Geografia e Estatística, RAMSAC CORS of Instituto Geográfico Nacional de la República Argentina, Arecibo Observatory, Low-Latitude Ionospheric Sensor Network (LISN), Canadian High Arctic Ionospheric Network, Institute of Geology and Geophysics, Chinese Academy of Sciences, China Meteorology Administration, Centro di Ricerche Sismologiche, Système d'Observation du Niveau des Eaux Littorales (SONEL), RENAG: REseau NAtional GNSS permanent - https://doi.org/10.15778/resif.rg, GeoNet - the official source of geological hazard information for New Zealand, Finnish Meteorological Institute, SWEPOS - Sweden, Hartebeesthoek Radio Astronomy Observatory, TrigNet Web Application, South Africa, Australian Space Weather Services, RETE INTEGRATA NAZIONALE GPS, Estonian Land Board, TU Delft, Western Canada Deformation Array, EUREF Permanent GNSS Network, GeoDAF: Geodetic Data Archiving Facility, African Geodetic Reference Frame (AFREF), Kartverket - Norwegian Mapping Authority, Geoscience Australia, IGS Data Center of Wuhan University, Pacific Northwest Geodetic Array, Nevada Geodetic Laboratory, Earth Observatory of Singapore, National Time and Frequency Standard Laboratory - Taiwan, and Korea Astronomy and Space Science Institute

Citations

Bilitza, D. (2018). IRI the international standard for the ionosphere. Adv. Radio Sci., 16 , 1–11. doi: 10.5194/ars-16-1-2018858

Bramley, E., & Peart, M. (1965). Effect of ionization transport on the equatorial f-region. Nature, 206 , 1245–1246.

Burrell, A. G., McDonald, S., Hickey, D., Burleigh, M., Nossa, E., Metzler, C. A., Dhadly, M., Tate, J. L., and Wagner, E. J. (2026). Next-generation Ionospheric Model for Operations -- validation and demonstration for space weather and research, 44(1), 303-329, doi: 10.5194/angeo-44-303-2026.

Burrell, A. G., Klenzing, J., Stoneback, R., & Pembroke, A. (2024, March). pysat/pysatmadrigal: v0.2.0 release [Software]. Zenodo. doi: 10.5281/zenodo.10823202

Forsythe, V., Servan-Schreiber, N., Burrell, A. G., & Valentine, H. C. (2025, November). victoriyaforsythe/pyiri: v0.1.3 [Software]. Zenodo. doi: 10.5281/zenodo.17546232900

Forsythe, V. V., Bilitza, D., Burrell, A. G., Dymond, K. F., Fritz, B. A., & Mc-Donald, S. E. (2024). Pyiri: Whole-globe approach to the international reference ionosphere modeling implemented in python. Space Weather , 22 (4), e2023SW003739. doi: 10.1029/2023SW003739904

Hanson, W. B., & Moffett, R. J. (1966). Ionization transport effects in the equatorial f region. Journal of Geophysical Research (1896-1977), 71 (23), 5559-5572. Retrieved from https://agupubs.onlinelibrary.wiley.com/doi/abs/10.1029/JZ071i023p05559 doi: https://doi.org/10.1029/JZ071i023p05559

Knudsen, D. J., Burchill, J. K., Buchert, S. C., Eriksson, A. I., Gill, R., Wahlund, J.-E., . . . Moffat, B. (2017). Thermal ion imagers and langmuir probes in the swarm electric field instruments. Journal of Geophysical Research: Space Physics, 122 (2), 2655-2673. Retrieved from https://agupubs.onlinelibrary.wiley.com/doi/abs/10.1002/2016JA022571 doi:https://doi.org/10.1002/2016JA022571

Martyn, D. F. (1955, January). Theory of Height and Ionization Density Changes at the Maximum of a Chapman-like Region, taking account of Ion Production, Decay, Diffusion and Tidal Drift. In Physics of the ionosphere (p. 254).

Mitra, S. (1946). Geomagnetic control of region F2 of the ionosphere. Nature, 158 (668).

Moffett, R., & Hanson, W. (1965). Effect of ionization transport on the equatorial f-region. Nature, 206 (4985), 705–706.

Rideout, W., & Cariglia, K. (n.d.). Cedar madrigal database [Database]. Retrieved from https://cedar.openmadrigal.org

Rideout, W., & Coster, A. J. (2006, May). Automated GPS processing for global total electron content data. GPS Solutions, 10 (3), 219–228. doi: 10.1007/s10291-006-0029-5983

Vierinen, J., Coster, A. J., Rideout, W. C., Erickson, P. J., & Norberg, J. (2016). Statistical framework for estimating gnss bias. Atmospheric Measurement Techniques, 9 (3), 1303–1312. Retrieved from https://amt.copernicus.org/articles/9/1303/2016/ doi: 10.5194/amt-9-1303-2016

Equatorial Ionization Anomaly (EIA)

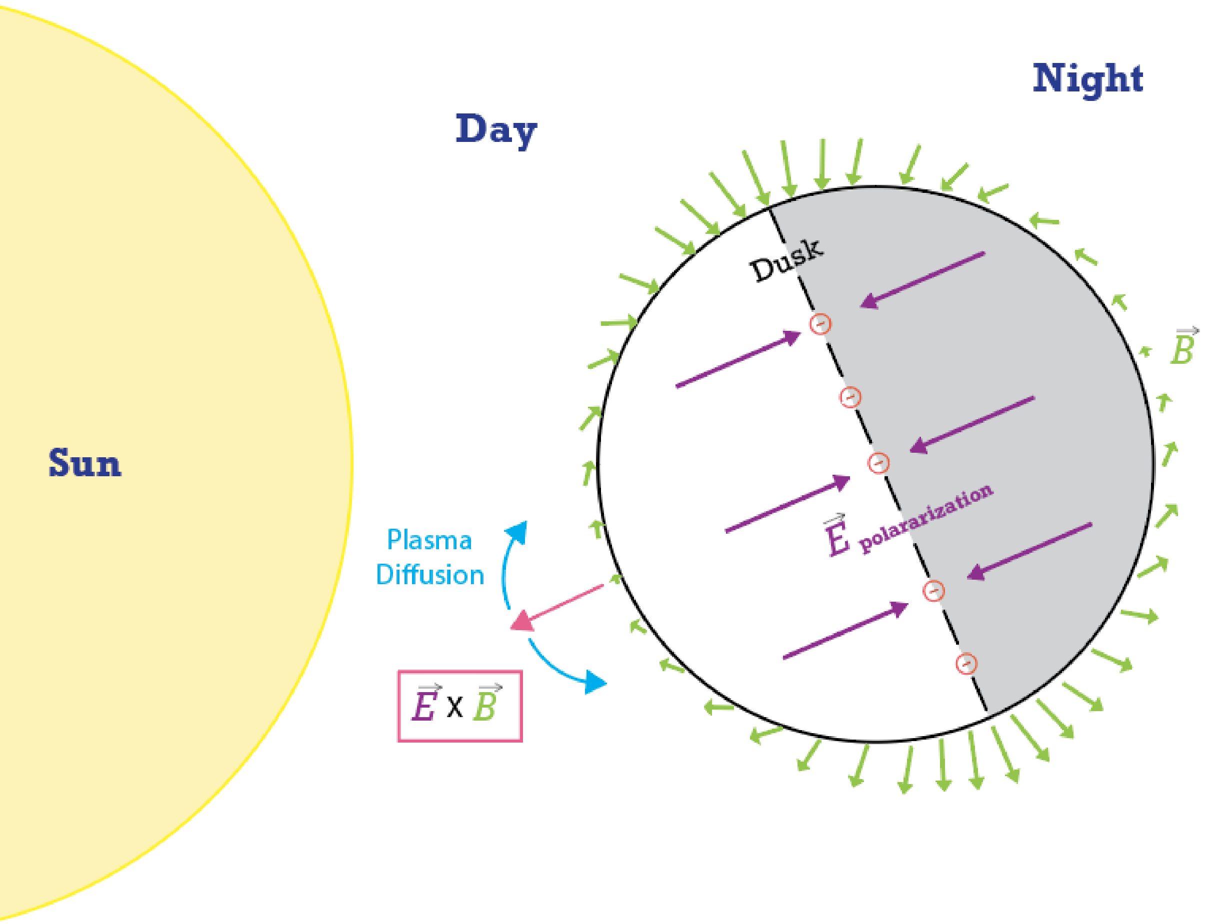

- Plasma builds up at the subsolar point and is displaced by ExB drift (e.g., Martyn, 1955) and plasma diffusion (e.g., Mitra, 1946)
- These processes act in conjunction along magnetic field lines at all latitudes and altitudes (Moffett & Hanson, 1965; Bramley & Peart, 1965; Hanson & Moffett, 1966)